

Janus Emulsion Solar Concentrators as Photocatalytic Droplet Microreactors

Pablo Simón Marqués, Bradley D. Frank, Aleksandr Savateev, and Lukas Zeininger*

Efficiently harvesting and conveying photons to photocatalytic reaction centers is one of the great obstacles in photocatalysis. To address this challenge, a new approach is reported that is based on employing biphasic complex emulsions as droplet-based solar concentrators. Specifically, substrates and photocatalysts are compartmentalized into the confined space of Janus emulsion droplets comprised of a hydrocarbon partially encapsulated inside fluorocarbon oil with a large refractive index contrast. Optical confinement of the incident light due to total internal reflection at the concave internal interface of the biphasic emulsion droplets leads to a strong increase of the light intensity inside the reaction medium. In addition, the high gas solubility within the outer fluorocarbon phase promotes oxygen delivery in photocatalytic oxidation reactions. Both effects mutually contribute to a strong performance increase of a series of homogeneous and heterogeneous photocatalytic reactions even under diffuse sunlight conditions.

In this context, complex emulsions, kinetically stabilized dispersions of two or more immiscible fluids in another phase-separated liquid medium, offer a versatile platform as they display tunable transmission properties, controllably adjustable internal droplet geometries, and large surface-to-volume ratios, promising an increased irradiation efficiency. Emulsification is a powerful, age-old technique for mixing and dispersing immiscible components within a continuous liquid phase and widely employed in organic synthesis.^[5] As such, emulsions are industrially deployed on the largest scale as they allow regulation of the viscosity and heat flux in chemical reaction cycles, present advantages such as easy processability, synthetic versatility, and relatively low cost and offer increased control over chemical

1. Introduction


Using sunlight energy for photocatalytic chemical activation and transformations of molecules represents a long-standing dream of society. Although photocatalytic reaction schemes offer great promise for an economically and environmentally sustainable transformation of molecules,^[1] current state-of-the-art technologies often suffer from drawbacks such as the requirement for high light intensities, long reaction times, and/or complicated equipment.^[2] The efficiency and scalability of a simple “flask in the sun” approach is hampered due to the typically high extinction coefficients of photoredox catalysts resulting in attenuation of photon transport and a limited light penetration inside the reaction vessel.^[3] As a result, large-scale practical applications require alternative new concepts for efficient harvesting and concentrating solar energy toward photocatalytic reaction centers.^[4]

reactions, e.g. due to molecular confinement, phase-selective partitioning of reagents or products, or for using the compartmentalization inside emulsion droplets to gain control of polymer molecular weight, viscosity, and heat flux.^[6]

Owing to their phase complexity and tunable internal geometries, multiphase emulsion droplets have been employed in a series of applications, including as structural templates for the generation of precision objects,^[7] for the encapsulation and release of components,^[8] and as reconfigurable optical elements. As for the latter, adjustment of the refractive indices of the constituent fluids in combination with gravitational alignment allows modulating the optical characteristics and to manipulate the pathway of light passing through these microscale elements, which endowed their establishment as tunable microlenses,^[9] and as refractory,^[10] or reflectory elements with iridescent colors and tunable angular emissive properties.^[11] Besides leveraging the optical properties of these functional colloidal components in optical applications, paints, displays, and sensors, we anticipated that complex emulsions offer rich opportunities for collecting and directing solar energy toward photocatalytic reaction centers.

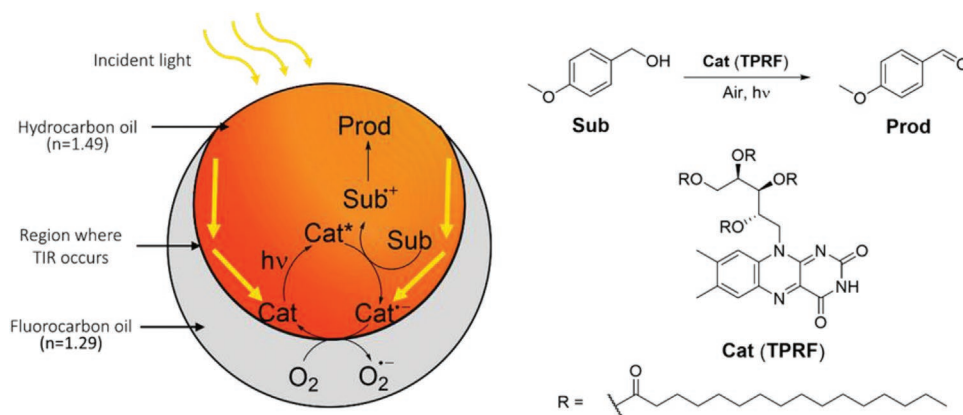
Given the structurally anisotropic nature of microscale Janus emulsions and that incident light can be reflected from the near edge of the concave internal interfaces, we hypothesized that liquid-compound microreactors comprised of high- and low-refractive-index media could serve as small, cheap, and transparent solar concentrators. We rationalized that light that enters the higher refractive index hydrocarbon phase containing a photocatalytic reaction mixture would be subjected to optical confinement, thereby increasing the light intensity

P. Simón Marqués, B. D. Frank, A. Savateev, L. Zeininger
Department of Colloid Chemistry
Max Planck Institute of Colloids and Interfaces
Am Muehlenberg 1, 14476 Potsdam, Germany
E-mail: lukas.zeininger@mpikg.mpg.de

 The ORCID identification number(s) for the author(s) of this article can be found under <https://doi.org/10.1002/adom.202101139>.

© 2021 The Authors. Advanced Optical Materials published by Wiley-VCH GmbH. This is an open access article under the terms of the Creative Commons Attribution License, which permits use, distribution and reproduction in any medium, provided the original work is properly cited.

DOI: 10.1002/adom.202101139



Scheme 1. Conceptual sketch of the working principle of Janus emulsion-based solar concentrators, used in this work. The complex emulsions were comprised of a phase-separated mixture of toluene (hydrocarbon oil) and HFE7500/FC43 (9:1; fluorocarbon oil) dispersed within an aqueous surfactant-containing (Zonyl-FS300; 1 wt%) continuous phase. Incoming light is directed and conveyed toward photocatalytic reaction centers, via total internal reflection (TIR) pathways at the internal interface of complex emulsions comprised of two fluids with a large refractive index contrast (left). Scheme of the photocatalytic oxidation of anisyl alcohol (Sub) to 4-methoxybenzaldehyde (Prod) and chemical structure of the flavin-based tetra-*O*-palmitoyl riboflavin (TPRF) photocatalyst (Cat) (right).

inside the molecularly crowded microenvironment of macroemulsion droplets (Scheme 1).

2. Results and Discussion

To test our hypothesis, we first opted for a photochemical oxidation of benzyl alcohols to corresponding aldehydes, mediated by flavin as a model transformation to evaluate the reaction parameters. To promote selective partitioning within the hydrocarbon phase of the emulsion droplets, we employed a tailor-made organo-soluble flavin-derivative (tetra-*O*-palmitoyl riboflavin; hereafter referred to as TPRF) as photocatalyst, synthesized via straightforward esterification of riboflavin (vitamin B2) using palmitoyl chloride.^[12]

To investigate the photocatalytic performance, we first tested a photocatalytic oxidation of anisyl alcohol under homogeneous standard conditions.^[13] Here we dissolved the substrates (0.015×10^{-3} M) and photocatalysts (TPRF; 10 mol%) in toluene and irradiated a thin layer (≈ 200 μm) of the reaction mixture using a LED lamp (74 mW cm^{-2}) at 25 $^{\circ}\text{C}$ for 1 h. The reaction yielded 4-methoxybenzaldehyde 2a in 38% yield proving the energy demand for this organic transformation (Table 1, entry 1).

However, when we compartmentalized the reaction mixture inside bi-phasic emulsion microreactors, we observed a dramatic yield increase resulting in an almost quantitative conversion (99%) within the same reaction time (1 h). In our approach, we compartmentalized an equimolar reaction mixture inside the hydrocarbon phase of complex emulsion droplets, comprised of a 1:1 volume mixture of toluene as the internal phase partially encapsulated within a fluorocarbon oil phase (mixture of HFE-7500 and FC-43). To this end, substrates and photocatalysts were pre-dissolved inside the toluene phase prior to emulsification of the oil mixture within an aqueous surfactant solution (Zonyl-FS300 1 wt%) using an established thermal phase separation approach.^[14] The internal shape of droplets generated using this method is dependent on the balance of

interfacial tensions acting at the individual interfaces, and as a result, lowering the fluorocarbon-water interfacial tension using the fluorocarbon surfactant Zonyl-FS300 yields Janus emulsions in an close to encapsulated morphology.^[15] These droplet microreactors aligned by gravity with the denser fluorocarbon phase placed at the bottom. Irradiation of gravity-aligned single layers of such polydisperse Janus emulsions (average diameter = 126 μm) gave conversions of ≈ 51 % after 30 min (entry 2) and almost quantitative yields (99%) after 1 h (entry 3), both vastly exceeding the yields obtained using the standard conditions (entry 1) or within single phase emulsion droplets (Table S1, Supporting Information). To isolate the products, droplets were de-emulsified through addition of salt, followed by separation of the fluorocarbon and water phase via extraction with hexane.

Motivated by these findings, we next tested this model photocatalytic reaction under ambient solar irradiation. Whereas under sunlight conditions half of the substrate of a reference reaction in toluene remained unreacted (entry 4), GC analysis of the transformation carried out inside the droplet microreactors showed complete conversion within 1 h (entry 5), confirming the potential application of the complex emulsions as

Table 1. Investigation and optimization of reaction conditions (anisyl alcohol 1a (0.015 mmol), tetra-*O*-palmitoyl riboflavin (TPRF; 10 mol%), 25 $^{\circ}\text{C}$).

Entry	System	Irradiation	Time [h]	Yield [%]
1	Homogenous	461 nm	1	38
2	Emulsion thin layer	461 nm	0.5	51
3	Emulsion thin layer	461 nm	1	99
4	Homogenous	Sunlight	1	53
5	Emulsion thin layer	Sunlight	1	99
6	Emulsion thin layer	Dark	1	<5
7	Emulsion multilayer	461 nm	1	76
8	Emulsion (Janus)	461 nm	1	85

solar concentrator microreactors for sunlight-powered chemical reactions.

Control experiments outlined the relevance of sufficient light penetration inside the droplets as a driving force for the performance increase (entry 6). While experiments performed inside droplets organized in thin-layers yielded 2a quantitatively, a decrease of the light penetration depths by performing the reaction in droplet multilayers lowered the obtained yields to 76% (entry 7). In contrast, when maintaining adequate incident light penetration toward the droplet microreactors, the general methodology could also be applied under up-scaled reaction conditions (30-times increased reaction volume; Figure S11 and Table S1, Supporting Information).

Beside the intensity of incident light, the internal droplet morphology played a significant role in the photocatalytic performance. The internal droplet morphology can be controllably altered by changing the force-balance of surface tensions. As such, we generated droplets that exhibit a hemispherically layered internal “perfect” Janus morphology via additional stabilization of the hydrocarbon-water interface using sodium dodecylsulfate surfactants (SDS) (Figure S10, Supporting Information). When compared to droplets in a more encapsulated internal morphology, droplets in perfect Janus configuration yielded lower conversion of the substrate (entry 8), which outlined the contribution of a concave-shaped internal droplet interface.

To understand the underlying optical phenomena inside these double emulsion solar concentrators, we modeled the trajectories of noncollimated incident light using a customized nonsequential ray-tracing algorithm in MATLAB (for details see

Supporting Information). To emulate generic lighting conditions, we arranged 60 million rays above the droplet with randomized starting directions and locations both to the left and right of the droplet to include off axis incident rays (Figure S2, Supporting Information). The pathways of the light from rays that enter the hydrocarbon phase of the droplets were traced and the sum of the individual ray amplitudes was mapped to display the light intensity distribution throughout the droplets. Our computational simulations revealed a strong anisotropic light intensity distribution inside the droplets with significantly higher light intensities inside the hydrocarbon phase in proximity to the internal interface of the complex emulsions. The large refractive index contrast between the hydrocarbon ($n_H = 1.49$) and fluorocarbon ($n_F = 1.29$) phase of the droplets produces reflectivity and light rays that intersect the internal hydrocarbon/fluorocarbon interface at an angle larger than the critical angle for total internal reflection (TIR) $\theta_c = \sin^{-1}(n_F/n_H) = 60^\circ$ are guided along the internal droplet interface. This effect could also be observed experimentally, when the emulsion droplets comprised of two fluids with a large refractive index contrast were viewed under a bright-field microscope. Due to optical confinement of incoming light horizontal and vertical micrographs of the droplets displayed a characteristic dark ring in proximity to the internal droplet interfaces (Figure 1a,b). As our calculations revealed, the latter indicated the region where incoming light rays are subject to TIR trajectories. The calculations also demonstrate that droplets with a concave internal interface can significantly enhance the distribution and intensity of incoming light within the complex emulsion microreactors (Figure 1c), whereas this effect is

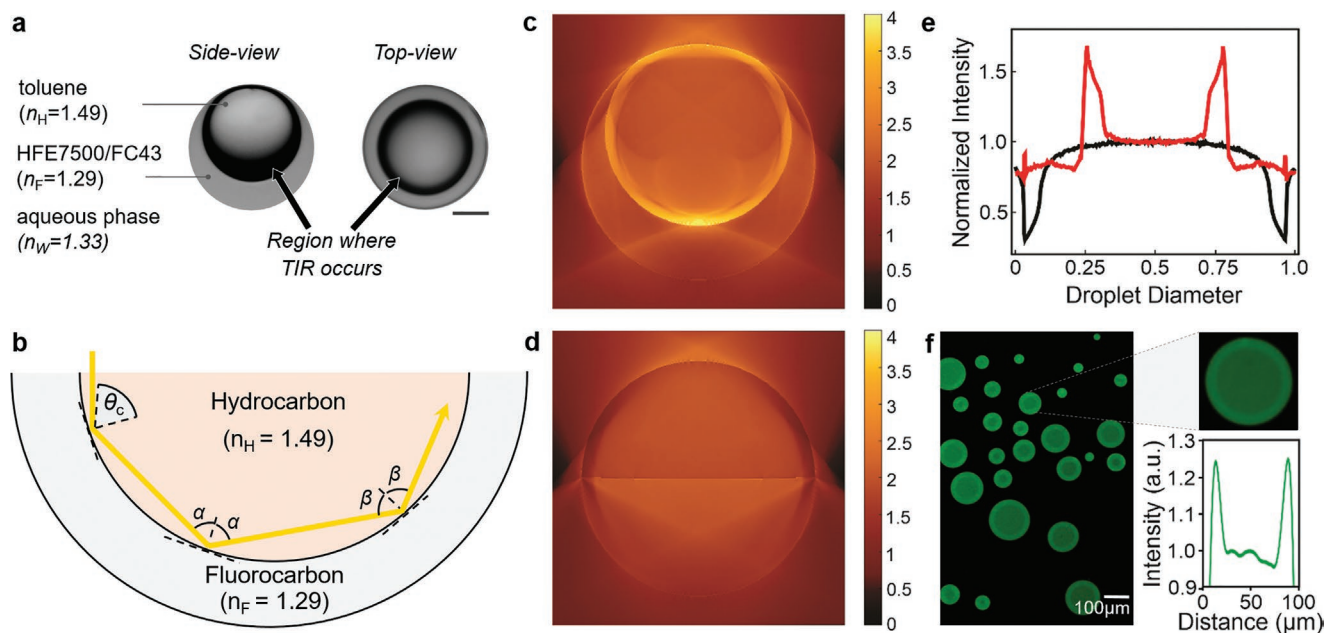


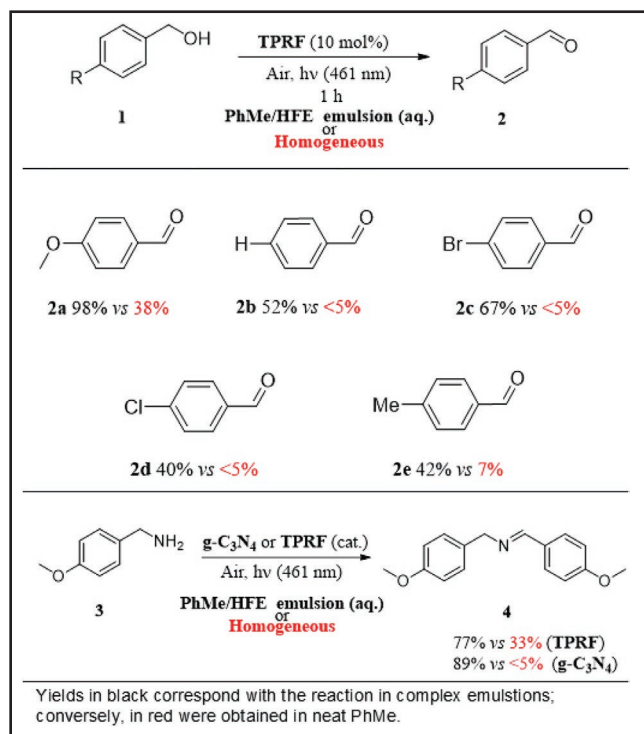
Figure 1. Modeling of emulsion droplet-based solar concentrators. a) Side- and top-view optical bright-field micrographs of double emulsion droplets showing a characteristic dark ring close to the internal droplet interface indicating the region where total internal reflection (TIR) of incident light occurs. Scale bar, 25 μm . b) Diagram of an incident light ray undergoing TIR at the concave internal hydrocarbon–fluorocarbon interface. c) Two-dimensional computational model of the light intensity distribution inside a close to encapsulated Janus emulsion droplet. d) Light intensity map obtained for a droplet in a “perfect” Janus morphology under the same conditions. e) Plot of the light intensity along a cross-section ($0.8 \times r$ from the top) of encapsulated (red) and Janus (black) droplets derived from the raytracing calculations. f) Confocal fluorescence micrograph of a cross-section of tetra-*O*-palmitoyl riboflavin (TPRF) dyed complex two-phase emulsion droplets, which display an increased light emission close to the internal droplet interface.

significantly reduced in droplets in a “perfect” Janus configuration (Figure 1d). A comparison of the light intensity maps along a cross-section of the calculated “perfect” Janus and biphasic emulsion droplets exhibiting a concave-shaped internal interface revealed the strong differences in incident light intensity (Figure 1e). Fluorescence micrographs of dyed (TPRF) biphasic emulsion droplets corroborated the theoretical results, as a locally enhanced excitation of photoactive molecules close to the internal droplet interface can be attributed to the increased excitation light intensity close to the internal droplet interface (Figure 1f and Figure S1, Supporting Information).

In addition to the optical phenomena underlying the significant increase in photocatalytic performance, we next investigated the capability of the adjacent fluorocarbon phase to serve as an oxygen reservoir promoting the oxygen concentration in the proximity of the active catalytic reaction centers. Within the parameters of net-oxidative photocatalytic reactions, the availability of an external oxidant plays an essential role. Perfluorocarbons are well known for their high oxygen dissolving capacity, which have been exploited in a number of applications, including liquid ventilation, drug delivery, catalysis, or blood substitutes.^[16] To reveal the contribution of the adjacent fluorocarbon phase inside the droplet microreactors to the photocatalytic performance increase we compared the performance of a reaction inside droplets comprised of a fluorocarbon phase that was stored under ambient conditions to that inside droplets comprising an oxygen presaturated fluorocarbon phase and observed a 2.6-fold increase in the reaction rate ($k = 5.35 \times 10^{-2} \text{ min}^{-1}$ versus $k = 2.08 \times 10^{-2} \text{ min}^{-1}$). In contrast, changes in the atmospheric conditions of the bulk emulsions had only insignificant influence on the overall catalytic performance (Figure S16, Supporting Information). To this end, we observed only a marginal performance increase ($\approx 9\%$) when the whole emulsion was stored under oxygen conditions but, on the other hand, still obtained comparable reaction rates when placing the as-made emulsion microreactors under inert gas atmosphere confirming the dominant role of the fluorocarbon phase in providing sufficient oxygen to regenerate the photocatalyst.

To investigate a potential general utility of the Janus emulsion solar concentrator microreactors to promote also the performance of other photocatalytic transformations, we next set out to determine the scope of the flavin-mediated photochemical oxidation of benzyl alcohols to corresponding aldehydes (Table 2). To this end, a series of substrates with electron-donating or –withdrawing substituents were tested. Similar to our model reaction, a significant increase in conversion within a 1 h reaction time was observed when performing the reactions inside emulsion droplets as opposed to the mostly negligible performance under standard conditions in neat toluene. In an alternative reaction scheme, we tested the viability of the emulsion microreactor approach to increase also the performance of another photocatalytic reaction. As for the latter, we opted for a photocatalytic oxidation of 4-methoxybenzylamine 3 to the respective imine 4, performed under homogeneous as well as heterogeneous photocatalytic reaction conditions. Here, a photocatalytic oxidation in the presence of TPRF as homogeneous catalyst resulted in a conversion of 77% after 30 min, which surpassed the 33% conversion observed under

Table 2. Scope of the photocatalytic oxidations.



conventional conditions. The same photocatalytic reaction was then also performed using a heterogeneous carbon nitride photocatalyst ($\text{g-C}_3\text{N}_4$) pre-dispersed inside the droplet. Carbon nitrides hold great promise as an inexpensive metal-free heterogeneous photocatalyst due to advantages such as simple processability and cost-effective separation and recycling, however suffer even more from poor light penetration due to the light back-scattering by the suspended particles.^[17] As a result, an increase of the light penetration inside the reaction medium as achieved by employing the biphasic complex emulsion approach yielded 4 with 89% conversion as opposed to an only negligible conversion under conventional conditions, highlighting the compatibility of the Janus emulsion solar concentrator approach also toward heterogeneous photocatalytic reaction schemes.

3. Conclusion

In conclusion, in this manuscript a novel application of complex emulsions in the context of efficient solar energy harvesting was investigated. Biphasic complex emulsions comprised of two oils with a large refractive index contrast can enrich and distribute diffuse noncollimated incident light through total internal reflection trajectories and thereby convey photons to photocatalytic reaction centers compartmentalized inside the droplet microreactors. A strong correlation between the experimental data and computational model provided for an understanding of the underlying phenomena and served to explain the significantly increased performance of photocatalytic transformations when performed inside emulsion solar

concentrators. In combination with the ability of the adjacent fluorocarbon phase to act as an oxygen reservoir promoting the local oxygen concentration in the proximity of the active catalytic reaction centers, Janus emulsion microreactors offer opportunities to tune reaction rates and yields of both, homogeneous and heterogeneous photoredox catalytic reactions, resulting in an unprecedented, powerful, and cost-effective emulsion platform that offers multiple enticing opportunities for realizing more sustainable chemical transformations, as well as for the development of new and improved optical emulsion technologies, such as reflective coatings, transducers, and signal amplifiers in sensing devices, and dynamic microoptical components.

Supporting Information

Supporting Information is available from the Wiley Online Library or from the author.

Acknowledgements

The authors gratefully acknowledge funding through the “Experiment!” program of the Volkswagen (VW) foundation. The authors are also grateful for financial support from the Max-Planck Society and through the Emmy-Noether program of the German Research Foundation under grant no. ZE 1121/3 1.

Open access funding enabled and organized by Projekt DEAL.

Conflict of Interest

The authors declare no conflict of interest.

Data Availability Statement

Raytracing data for this study is available from the corresponding author. The customized MATLAB code used to implement the model is available for download from <https://github.com/snnagel/MultiPhaseDropletRaytracer>.

Keywords

complex emulsions, Janus emulsions, photocatalysis, ray-tracing, solar concentrators

Received: June 7, 2021
Revised: September 3, 2021
Published online: October 17, 2021

- [1] a) D. Durgalakshmi, R. Ajay Rakkesh, S. Rajendran, M. Naushad, *Principles and Mechanisms of Green Photocatalysis*, Springer International Publishing, Berlin **2020**; b) D. Ravelli, D. Dondi, M. Fagnoni, A. Albin, *Chem. Soc. Rev.* **2009**, *38*, 1999.
[2] a) F. Lévesque, M. J. Di Maso, K. Narsimhan, M. K. Wismer, J. R. Naber, *Org. Process Res. Dev.* **2020**, *24*, 2935; b) K. C. Harper, E. G. Moschetta, S. V. Bordawekar, S. J. Wittenberger, *ACS Cent. Sci.* **2019**, *5*, 109.

- [3] R. Acosta-Herazo, M. Á. Mueses, G. L. Puma, F. Machuca-Martínez, *Chem. Eng. J.* **2019**, *356*, 839.
[4] a) D. Cambié, J. Dobbelaar, P. Riente, J. Vanderspikken, C. Shen, P. H. Seeberger, K. Gilmore, M. G. Debije, T. Noël, *Angew. Chem.* **2019**, *131*, 14512; *Angew. Chem., Int. Ed.* **2019**, *58*, 14374; b) B. Pieber, M. Shalom, M. Antonietti, P. H. Seeberger, K. Gilmore, *Angew. Chem.* **2018**, *130*, 10127; *Angew. Chem., Int. Ed.* **2018**, *57*, 9976; c) Z. J. Wang, S. Ghasimi, K. Landfester, K. A. I. Zhang, *Adv. Mater.* **2015**, *27*, 6265; d) D. Cambié, F. Zhao, V. Hessel, M. G. Debije, T. Noël, *Angew. Chem.* **2017**, *129*, 1070; *Angew. Chem., Int. Ed.* **2017**, *56*, 1050; e) L. Zhang, Z. Zhu, B. Liu, C. Li, Y. Yu, S. Tao, T. Li, *Adv. Sci.* **2019**, *6*, 1900583.
[5] a) S. Narayan, J. Muldoon, M. G. Finn, V. V. Fokin, H. C. Kolb, B. K. Sharpless, *Angew. Chem.* **2005**, *117*, 3339; *Angew. Chem., Int. Ed.* **2005**, *44*, 3275; b) H. Gröger, O. May, H. Hüsken, S. Georgeon, K. Drauz, K. Landfester, *Angew. Chem.* **2006**, *118*, 1676; *Angew. Chem., Int. Ed.* **2006**, *45*, 1645; c) M. F. Ruiz-Lopez, J. S. Francisco, M. T. C. Martins-Costa, J. M. Anglada, *Nat. Rev. Chem.* **2020**, *4*, 459; d) A. Fallah-Araghi, K. Meguellati, J. Baret, A. El Harrak, T. Mangeat, M. Karplus, S. Ladame, C. M. Marques, A. D. Griffiths, *Phys. Rev. Lett.* **2014**, *112*, 028301.
[6] a) D. C. Dewey, C. A. Strulson, D. N. Cacace, P. C. Bevilacqua, C. D. Keating, *Nat. Commun.* **2014**, *5*, 4670; b) D. Sarker, *Pharmaceutical Emulsions: A Drug Developer's Toolbag*, John Wiley & Sons, West Sussex, UK **2013**; c) G. Dockx, S. Geisel, D. G. Moore, E. Koos, A. R. Studart, J. Vermant, *Nat. Commun.* **2018**, *9*, 4763; d) M. S. Chowdhury, W. Zheng, S. Kumari, J. Heyman, X. Zhang, P. Dey, D. A. Weitz, R. Haag, *Nat. Commun.* **2019**, *10*, 4546; e) X. Yan, R. M. Bain, R. G. Cooks, *Angew. Chem., Int. Ed.* **2016**, *55*, 12960; f) D. Guzey, D. J. McClements, *Adv. Colloid Interface Sci.* **2006**, *128*, 227.
[7] a) L. Ge, J. Cheng, D. Wei, Y. Sun, R. Guo, *Langmuir* **2018**, *34*, 7386; b) B. D. Frank, M. Antonietti, L. Zeininger, *Macromolecules* **2021**, *54*, 981; c) B. D. Frank, M. Perovic, S. Djalali, M. Antonietti, M. Oschatz, L. Zeininger, *ACS Appl. Mater. Interfaces* **2021**, *13*, 32510.
[8] a) B. J. Sun, H. C. Shum, C. Holtze, D. A. Weitz, *ACS Appl. Mater. Interfaces* **2010**, *2*, 3411; b) W. J. Duncanson, T. Lin, A. R. Abate, S. Seiffert, R. K. Shah, D. A. Weitz, *Lab Chip* **2012**, *12*, 2135.
[9] a) S. Nagelberg, L. D. Zarzar, N. Nicolas, K. Subramanian, J. A. Kalow, V. Sresht, D. Blankschtein, G. Barbastathis, M. Kreysing, T. M. Swager, M. Kolle, *Nat. Commun.* **2017**, *8*, 14673; b) L. D. Zarzar, J. A. Kalow, X. He, J. J. Walsh, T. M. Swager, *Proc. Natl. Acad. Sci. USA* **2017**, *114*, 3821.
[10] a) Q. Zhang, L. Zeininger, K. Sung, E. A. Miller, K. Yoshinaga, H. D. Sikes, T. M. Swager, *ACS Sens.* **2019**, *4*, 180; b) L. Zeininger, E. Weyandt, S. Savagatrup, K. S. Harvey, Q. Zhang, Y. Zhao, T. M. Swager, *Lab Chip* **2019**, *19*, 1327.
[11] a) A. E. Goodling, S. Nagelberg, B. Kaehr, C. H. Meredith, P. Ashley, M. Kolle, L. D. Zarzar, *Nature* **2019**, *566*, 523; b) L. Zeininger, S. Nagelberg, K. S. Harvey, S. Savagatrup, M. B. Herbert, K. Yoshinaga, J. A. Capobianco, M. Kolle, T. M. Swager, *ACS Cent. Sci.* **2019**, *5*, 789.
[12] a) R. Cibulka, *Eur. J. Org. Chem.* **2015**, *5*, 915; b) V. Mojr, E. Svobodová, K. Straková, T. Neveselý, J. Chudoba, H. Dvořáková, *Chem. Commun.* **2015**, *51*, 12036.
[13] H. Schmaderer, P. Hilgers, R. Lechner, B. Koenig, *Adv. Synth. Catal.* **2009**, *351*, 163.
[14] L. D. Zarzar, V. Sresht, E. M. Sletten, J. A. Kalow, D. Blankschtein, T. M. Swager, *Nature* **2015**, *518*, 520.
[15] S. Djalali, B. D. Frank, L. Zeininger, *Soft Matter* **2020**, *16*, 10419.
[16] a) L. C. Clark, F. Gollan, *Science* **1966**, *152*, 1755; b) R. M. Rodrigues, X. Guan, J. A. Iñiguez, D. A. Estabrook, J. O. Chapman, S. Huang, E. M. Sletten, C. Liu, *Nat. Catal.* **2019**, *2*, 407.
[17] a) S. Mazzanti, B. Kurpil, B. Pieber, M. Antonietti, A. Savateev, *Nat. Commun.* **2020**, *11*, 1387; b) Y. Markushyna, C. A. Smith, A. Savateev, *Eur. J. Org. Chem.* **2020**, *10*, 1294.